On Finding Energy-Minimizing Paths on Terrains

Zheng Sun, *Member, IEEE,* and John H. Reif, *Fellow, IEEE*

***Abstract*—In this paper, we discuss the problem of computing optimal paths on terrains for a mobile robot, where the cost of a path is defined to be the energy expended due to both friction and gravity. The physical model used by this problem allows for ranges of impermissible traversal directions caused by overturn danger or power limitations. The model is interesting and challenging, as it incorporates constraints found in realistic situations, and these constraints affect the computation of optimal paths. We give some upper- and lower-bound results on the combinatorial size of optimal paths on terrains under this model. With some additional assumptions, we present an efficient approximation algorithm that computes for two given points a path whose cost is within a user-defined relative error ratio. Compared with previous results using the same approach, this algorithm improves the time complexity by using 1) a discretization with reduced size, and 2) an improved discrete algorithm for finding optimal paths in the discretization. We present some experimental results to demonstrate the efficiency of our algorithm. We also provide a similar discretization for a more difficult variant of the problem due to less restricted assumptions.**

***Index Terms*—Computational geometry, mobile-robot motion planning, optimization, road vehicles.**

I. Introduction

A. Motivation and Related Work

With the growth of geographical information systems (GIS), now it is possible to find a terrain map (such as the one for Kaweah River basin shown in Fig. 1) for virtually any location in the world. The availability of these high-resolution maps makes computing energy-minimizing paths for mobile robots possible. However, despite the obvious potential applications in both commercial and military areas, there has not been enough interest in the energy-minimizing path problem, as compared with its practical significance in the real world. The extensively studied Euclidean shortest-path problems fail to capture some of the characteristics of optimal path planning for a mobile robot, such as the variance of the friction coefficient in different areas, the limitations of the driving force of the robot, and the stability of the robot on a steep plane.

Manuscript received February 23, 2004. This paper was recommended for publication by Associate Editor N. Amato and Editor S. Hutchinson upon evaluation of the reviewers' comments. This work was supported in part by the National Science Foundation ITR under Grant EIA-0086015 and Grant 0326157; in part by the National Science Foundation QuBIC under Grant EIA-0218376 and Grant EIA-0218359; in part by the Defense Advanced Research Projects Agengy/Air Force Office of Scientific Research under Contract F30602-01-2-0561; and in part by the Research Grant Council under Grant HKBU2107/04E. This paper was presented in part at the IEEE International Conference on Robotics and Automation, Taipei, Taiwan, R.O.C., September 2003.

Z. Sun is with the Department of Computer Science, Hong Kong Baptist University, Kowloon, Hong Kong (e-mail: sunz@comp.hkbu.edu.hk).

J. H. Reif is with the Department of Computer Science, Duke University, Durham, NC 27708 USA (e-mail: reif@cs.duke.edu).

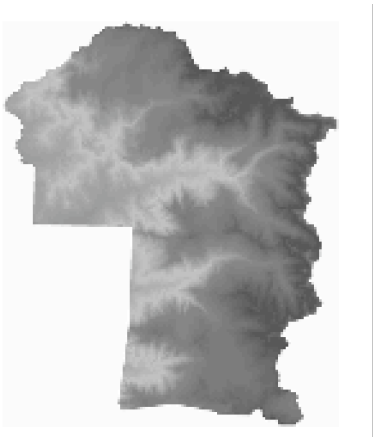

Fig. 1. Terrain map of Kaweah River basin.

In this paper, we study the problem of optimal path planning on terrains for a mobile robot. Our work is based on the model introduced by Rowe and Ross [1]. In their model, the *cost* of any path on the surface of a terrain is defined to be the energy loss due to both friction and gravity. The goal is to find an *optimal path*, a path with the minimum energy loss between given source and destination points s and t. This model adds anisotropism to optimal path planning by taking into consideration impermissible traversal directions resulting from overturn danger or power limitations. This problem is a generalization of the more extensively studied weighted-region optimal-path problem (see [2]–[11] or survey [12]), yet conceivably more difficult.

Although this model addresses some of the characteristics of optimal path planning for mobile robots that are not considered by Euclidean shortest-path problems, it still does not take into consideration nonholonomic constraints found in real contexts. We refer readers to [13] for a review of works on nonholonomic motion planning.

Rowe and Ross [1] studied the characteristics of optimal paths on terrains; they showed that there are only four ways that an optimal path could traverse a terrain face. They also provided rules for transition on the boundary edges for each combination of the four traversal types. Rowe and Kanayama [14] applied the same model to the surface of a vertical-axis ideal cone. In this case, there are 22 ways that an optimal path could traverse a conic surface patch. They also provided an approximation algorithm that uses these characteristics; this approximation algorithm is able to produce approximate optimal paths much smoother than the ones found by the traditional approximation algorithm using grid-based discretization. Rowe [15] later generalized their work to other path-planning problems with anisotropic cost functions, such as path planning for a missile in a three-dimensional space.

***Preprint of paper appearing* in IEEE Transaction on Robotics, Volume: 21, Issue: 1, February 2005, pages 102-114.**

Lanthier *et al.* [16] developed an approximation algorithm using a traditional discretization approach. By placing discrete points (called *Steiner points*) on the boundaries of terrain faces and interconnecting these points by edges with appropriate weights, they reduced the original optimal-path problem in a continuous geometric space to computing an *optimal discrete path* (a path with the minimum total weight) in a graph $\mathcal{G}$; the latter problem can be solved by a number of existing algorithms. The optimal discrete path found is then converted to a path in the original continuous space as an approximate solution. This discretization approach is also used for the weighted-region optimal-path problem (see [7]–[9] and [11]), as well as the optimal-path problem in the presence of flows (see [17]).

Other related work includes [18] and [19].

B. Our Results

We provide a couple of complexity results on the combinatorial size of optimal paths on terrains under this model. We show that any optimal path on a weighted terrain contains $O(n^2)$ segments. Here, n is the number of faces in the terrain. With the introduction of anisotropism, however, we can construct a terrain with specified points s and t such that any optimal path connecting s and t contains an exponential number of segments. These complexity results not only are of theoretical interest, but also have implications on the implementation of approximation algorithms, as we will explain in Section III.

Lanthier *et al.* [16] used Dijkstra's algorithm to compute an optimal discrete path in $\mathcal{G}$. If m Steiner points are placed on each boundary edge, their approximation algorithm has a time complexity of $O(nm^2 + nm\log(nm))$. We prove that the BUSHWHACK algorithm [8], [20], originally designed for the weighted-region optimal-path problem, can be applied to this problem as well, and therefore, an optimal discrete path in $\mathcal{G}$ can be computed in $O(nm\log(nm))$ time. BUSHWHACK is a discrete search algorithm that can efficiently compute optimal discrete paths by exploiting the geometric properties of the discretization. We also show that the discretization used by [16] can be reduced while still guaranteeing the same asymptotic error bound as in [16]. By combining this discretization of reduced size with the BUSHWHACK algorithm, our approximation algorithm not only has an improved time complexity over the result in [16], but also is less dependent on various geometric parameters, such as the minimum angle between two adjacent boundary edges of a terrain face, and the maximum angle of a special range. These observations are supported by the experimental results presented in Section VI.

We extend our work to difficult terrains containing steep terrain faces on which a robot can only move downhill. In this case, the optimal path planning is even more challenging, as a terrain face not only can have different cost metrics in various directions, but also may become an "anisotropic obstacle" that blocks any upward movement of a robot.

C. Notations and Organization of the Paper

For any path p on the surface of a terrain, we use $|p|$ to denote the Euclidean length of p, and use $||p||$ to denote the cost of p, i.e., the total energy loss for the robot to traverse p. For two points v_1 and v_2 on p, we use $p[v_1v_2]$ to denote the subpath of p between v_1 and v_2. For any two points v_1 and v_2 in the same terrain face r, we say that a path p connecting v_1 and v_2 is *face-wise optimal* if it is a minimum-cost path among all paths that lie entirely inside r, and define the *region distance* $d_r(v_1, v_2)$ from v_1 to v_2 to be the cost of p.

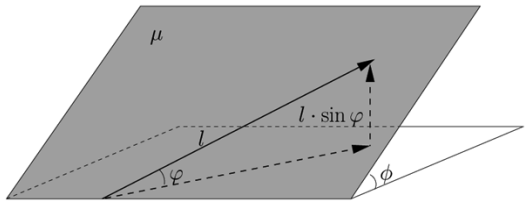

Fig. 2. Energy cost.

The rest of the paper is organized as follows. Section II describes the energy model used for our problem, as well as the discretization method for converting a terrain into a directed weighted graph by adding Steiner points on boundary edges. Section III presents a couple of upper- and lower-bound results on the combinatorial size of optimal paths on terrains. In Section IV, we provide an efficient approximation algorithm based on the discretization method described in Section II. Section V provides a similar discretization for the same model, but under less restricted assumptions. In Section VI, we provide some details of our implementation, as well as experimental results. Section VII concludes the paper with some open problems.

II. Preliminaries

A. Physical Model

We now describe the energy-cost model first developed by Rowe and Ross [1]. Let r be a terrain face with a gradient of ϕ, and let μ be the friction coefficient between the mobile robot and the surface of r. Following the notation of [16], we define $w = \mu \cdot \cos\phi$ to be the "weight" of r. For a robot traveling on r with an inclination angle of φ (as shown in Fig. 2), the energy cost is defined to be

$$C = mg(\mu\cos\phi + \sin\varphi) \cdot l = mg(w + \sin\varphi) \cdot l \quad (1)$$

where mg is the weight of the robot, and l is the traveled distance. According to Rowe and Ross [1], "This formula was confirmed experimentally within 1% for wheeled vehicles on slopes of less than 20% in [21]."

The problem is to find an energy-minimizing path from a given source point s to a given destination point t. The model assumes no acceleration when the robot is moving, and no energy cost for making turns. In the remainder of this paper, we assume that each terrain face is a triangular region, and that source s and destination t are vertices of some terrain faces. We use n to denote the total number of all terrain faces.

There are three *impermissible (angular) ranges* defined for each terrain face, as shown in Fig. 3. The first one is the *impermissible force range*, which indicates the range of uphill traversal directions that are too steep for a robot to climb. The other two are the *sideslope overturn ranges*, which include the forbidden directions that can cause overturn, as the projection of the robot's center of gravity falls outside the convex hull of the

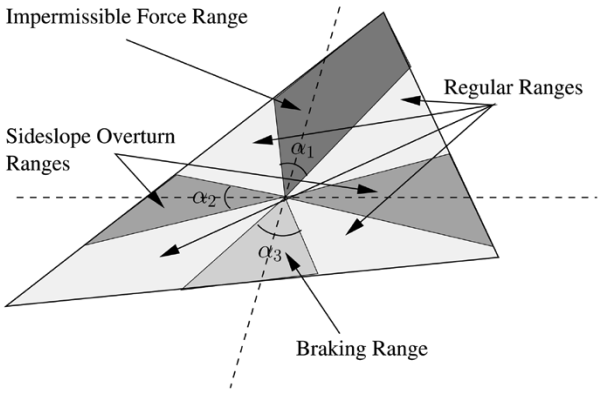

Fig. 3. Impermissible, braking, and regular (angular) ranges.

support points. Each boundary angle of an impermissible range is called a *critical impermissibility angle*.

Another special case occurs when a robot is traveling downhill with such an inclination angle φ that $w + \sin\varphi < 0$. This will cause the robot to gain energy and accelerate. Therefore, the robot has to apply a braking force of $-mg(w + \sin\varphi)$ to avoid acceleration. The range in which the robot has to use a braking force is called a *braking range*. The two boundary angles of the braking range, *critical braking angles*, can be computed by finding the solution φ_0 for the following equation:

$$w + \sin\varphi = 0. \tag{2}$$

The robot expends no energy when traveling in a direction inside the braking range, as the energy gained by going downhill is exactly offset by the energy expended for braking.

We call the impermissible force range, the sideslope overturn ranges, and the braking range *special ranges* of a terrain face. These special ranges are fixed for all points in that face. We define the *angle* of a range to be the angle between the two rays defining the boundary of the range. Let α_1, α_2, and α_3 be the angles of the impermissible force range, each sideslope overturn range, and the braking range, respectively. There are four *regular ranges*, each of which is between two adjacent special ranges. The energy-cost formula $mg(w+\sin\varphi)\cdot l$ only applies to the case when a robot is traveling in a direction inside a regular range.

Any feasible path consists of only segments whose directions are inside regular and braking ranges. To *effectively* move in a direction inside an impermissible range, a robot has to take a zigzag path with alternating directions that are inside regular or braking ranges. It is, therefore, implicitly assumed that a robot can freely switch between two directions inside regular ranges, even if there is an impermissible range in between. In particular, if the impermissible range is a sideslope overturn range, we assume that the robot can rotate sufficiently quickly to avoid overturn.

We say a range is *degenerate* if the size of the range is zero. A regular range can be degenerate if the two neighboring special ranges overlap with each other. In particular, if the braking range overlaps with the two sideslope overturn ranges, not only would the two adjacent regular ranges be degenerate, but also the *actual* braking range would be reduced; its boundary would be determined by the boundary angles of the two sideslope overturn ranges, instead of by (2).

A terrain face r is *regular* if all four special ranges are degenerate inside r; otherwise, r is *irregular*. If all the faces of a terrain are regular, we say that it is a *regular terrain*; otherwise, it is an *irregular terrain*.

In this paper, we mainly consider the optimal-path problem on irregular terrains. In particular, we are interested in the case where the angle of one of the special ranges is close to π. As we shall see later in this paper, the closer the size of a special range is to π, the larger the difference in cost metrics can be between two directions inside that range.

An irregular terrain face r is *totally traversable* if it is always possible to travel between two points in r through a (straight or zigzag) path that lies entirely inside r. This can be guaranteed if the two upper regular ranges are not degenerate, which means $\alpha_1 + \alpha_2 < \pi$. Otherwise, the impermissible force range of r would overlap with the two sideslope overturn ranges, forming a combined impermissible range with an angle equal to $\pi + \alpha_2$. For any direction $\overrightarrow{vv'}$ inside this range, there is no feasible path connecting v and v' that lies entirely inside r, as $\overrightarrow{vv'}$ cannot be expressed as a nonnegative linear combination of permissible directions. However, the braking range and/or the two lower regular ranges are not degenerate (as $\alpha_2 < \pi$), and therefore, there will still be permissible (downhill) traversal directions inside r. In this case, r is *partially traversable*. We say that a terrain is a *totally traversable terrain* if each terrain face is totally traversable; otherwise, it is a *partially traversable terrain*.

B. Construction of Graph $\mathcal{G}$

In the following, we show that we can construct a graph $\mathcal{G}$ in such a manner that, for any discrete path p from s to t in $\mathcal{G}$, there exists a path p' from s to t in the original continuous space with the same cost. Furthermore, p' can be computed from p in time linear to the combinatorial size of p'. Here we assume that the robot always translates along straight lines and rotates at the same position to achieve path optimality. In Section IV, we will show that the BUSHWHACK algorithm can be applied to $\mathcal{G}$ to compute an optimal discrete path.

Following the approach of Lanthier *et al.* [16] for the same problem, we discretize the original space by introducing Steiner points on boundary edges. For each terrain face r, we add a number of Steiner points on each boundary edge of r. We construct a graph $\mathcal{G}$ that includes all Steiner points and vertices as nodes. For any two such nodes v, v' on the boundary of r, we add a directed edge $\overline{vv'}$ in $\mathcal{G}$.

One difference between the weighted-region optimal-path problem and this problem is that edge $\overline{vv'}$ does not necessarily represent the straight-line path from v to v'. In particular, if direction $\overrightarrow{vv'}$ is inside one of the impermissible ranges, the straight-line path from v to v' is not allowed, according to the physical model we defined above. In this case, edge $\overline{vv'}$ represents a face-wise optimal path connecting v and v'. Edge $\overline{vv'}$ still represents the straight-line path from v to v' if it is in a braking or regular range. In all cases, $\overline{vv'}$ is assigned a weight $d_r(v, v')$ equal to the cost of the path it represents.

Now we consider how to compute the weight of edge $\overline{vv'}$. Let φ be the inclination angle of vector $\overrightarrow{vv'}$, and let l be the length of $\overline{vv'}$. By (1), the energy-cost formula is $mg(w+\sin\varphi)\cdot l$ for traveling from v to v' following a straight line, if φ is in a regular range. The first part $mg\cdot w\cdot l$ of the formula represents the energy expended due to the force of friction (friction cost), whereas the second part $mg\cdot\sin\varphi\cdot l$ represents the energy expended due to gravity (gravity cost). The total gravity cost for traveling from s to t is always the altitude difference between the two points, regardless of the path taken. Therefore, for the purpose of computing optimal paths we can extract the gravity cost from the cost formula. This leads to a simplified model, in which the cost of traveling for distance l with an inclination angle of φ is $mg\cdot w\cdot l$ (if φ is in a regular range). Similarly, if φ is in the braking range, the energy cost is zero for the robot. Therefore, in the simplified model, after removing the (negative) gravity cost of $mg\cdot\sin\varphi\cdot l$, the cost formula becomes $-mg\cdot\sin\varphi\cdot l$, which is the energy cost for braking. (Note that the cost is a positive value, as $\varphi<0$ in the braking range.)

In the following discussion, whenever we refer to the cost of a path, we mean the cost defined by the simplified model. This strategy is also used by [16]. With the simplified model, we have the following properties for face-wise optimal paths.

Property 1: Let v, v' be two points in a terrain face r. Let α be the angle of the range to which $\overrightarrow{vv'}$ belongs, and let θ be the angle between $\overrightarrow{vv'}$ and the ray bisecting the range. Then:

1) if direction $\overrightarrow{vv'}$ is inside a regular range, the face-wise optimal is the straight-line path $\overline{vv'}$, and the cost is $d_r(v,v')=mg\cdot w\cdot|\overline{vv'}|$;
2) if direction $\overrightarrow{vv'}$ is inside an impermissible range, any zigzag path with alternating directions of the two critical impermissibility angles of the range is face-wise optimal, and the cost is $d_r(v,v')=mg\cdot w\cdot|\overline{vv'}|\cdot(\cos\theta)/(\cos(\alpha/2))$;
3) if direction $\overrightarrow{vv'}$ is inside the braking range, any path whose traversal direction remains in the braking range is face-wise optimal, and the cost is $d_r(v,v')=-mg\cdot\sin\varphi\cdot|\overline{vv'}|=-mg\cdot\sin\varphi_0\cdot(\sin\varphi)/(\sin\varphi_0)\cdot|\overline{vv'}|=mg\cdot w\cdot|\overline{vv'}|\cdot(\cos\theta)/(\cos(\alpha/2))$.

The above formulae reveal two properties of face-wise optimal paths: 1) $d_r(v,v')$ can be stated in a uniform form for both impermissible ranges and the braking range, although α may represent different values; and 2) inside each special range, $d_r(v,v')$ is proportional to $|\overline{vv'}|\cdot\cos\theta$, the Euclidean length of the projection of $\overline{vv'}$ on the ray bisecting the range.

III. Upper Bound on Number of Segments of an Optimal Path

In Section II, we showed how to construct a graph $\mathcal{G}$ from a terrain. $\mathcal{G}$ is totally dependent on the discretization, i.e., the placement of Steiner points on boundary edges. An easy-to-implement discretization scheme is the uniform discretization, which places Steiner points with an equal distance between them on each boundary edge. For each terrain face r, we can properly choose the distance between two adjacent Steiner points on boundary edges of r, so that, for any crossing segment in r with cost C, there exists a neighboring *approximation segment* (a segment that connects two Steiner points/vertices) with cost $C+\epsilon$, for some user-specified ϵ. Therefore, for any optimal path with cost C_{opt}, there exists an approximate optimal path, which consists entirely of approximation segments, with a total cost of no more than $C_{\text{opt}}+k\cdot\epsilon$, where k is the number of segments of the optimal path.

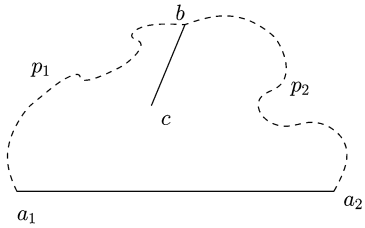

Fig. 4. *Lemma 1* for planar space.

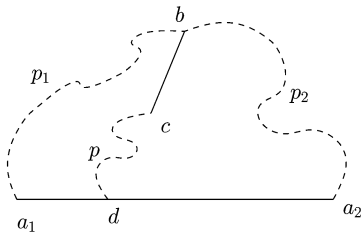

Fig. 5. *Lemma 2* for terrain.

To construct a uniform discretization that has a constant (additive) error bound, we need to find an upper bound on the number of segments for all optimal paths.

We first consider the case of regular terrains. Recall that any terrain face in a regular terrain has no impermissible or braking range. Therefore, finding an optimal path on a regular terrain is equivalent to the weighted-terrain optimal-path problem.

Mitchell and Papadimitriou [4] showed that an optimal path in a weighted planar subdivision has $O(n^2)$ segments. Their proof is generally applicable to the weighted-terrain case, except that the proofs of two key "shortcut lemmas" [4, Fact 1 and Fact 2] need to be strengthened. The proofs use the following basic lemma.

Lemma 1: As shown in Fig. 4, let a_1, a_2, and b be three points in a $2\mathcal{D}$ space, and let p_1 and p_2 be two paths connecting b with a_1 and a_2, respectively. If c is a point such that segment $\overline{bc}$ lies entirely inside the region bounded by p_1, p_2 and line segment $\overline{a_1a_2}$, then $|p_1|+|p_2|\geq|\overline{bc}|$, where $|p_i|$ is defined to be the Euclidean length of path p_i.

This lemma is no longer valid on a terrain. Even though line segment $\overline{bc}$ is inside the terrain area bounded by path p_1, p_2 and $\overline{bc}$ on the surface of the terrain, the above inequality may not hold, as the elevation difference between b and c can be arbitrarily large, and so is the Euclidean length of segment $\overline{bc}$. (Note that here segments $\overline{bc}$ and $\overline{a_1a_2}$ are not necessarily inside the same terrain face.) We need the following alternative basic lemma.

Lemma 2: As shown in Fig. 5, let a_1, a_2, and b be three points in a $3\mathcal{D}$ space, and let p_1 and p_2 be two paths connecting b with a_1 and a_2, respectively. Let d be a point on line segment

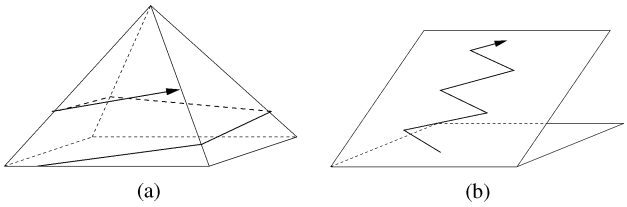

Fig. 6. Two noninteresting cases of long paths. (a) A zigzag path on one terrain face. (b) A zigzag path on multiple terrain faces.

$\overline{a_1a_2}$. Then, for any point c in the space and any path p connecting c and d, $|p_1| + |p_2| + |p| \geq |\overline{bc}|$.

Proof: Refer to Fig. 5. By using the triangle inequality three times, we have the following inequalities:

$$|p_1| + |\overline{a_1d}| + |p| \geq |\overline{bc}|$$
$$|p_2| + |\overline{a_2d}| + |p| \geq |\overline{bc}|$$
$$|p_1| + |p_2| \geq |\overline{a_1a_2}|.$$

Adding these three inequalities up, we have $2(|p_1|+|p_2|+|p|)+|\overline{a_1d}|+|\overline{a_2d}| \geq 2|\overline{bc}|+|\overline{a_1a_2}|$, and therefore, $|p_1|+|p_2|+|p| \geq |\overline{bc}|$, as $|\overline{a_1d}| + |\overline{a_2d}| = |\overline{a_1a_2}|$. ■

Note that for the terrain case, we need an extra term $|p|$ to bound $|\overline{bc}|$. Therefore, to adopt Mitchell and Papadimitriou's proof technique to the weighted-terrain case, the proofs of the two shortcut lemmas need to be tightened. We leave the descriptions, as well as the modified proofs of the two shortcut lemmas, in Appendix A due to their lengths. Here we just state our result in the following theorem.

Theorem 1: Any optimal path on a regular terrain has $O(n^2)$ segments.

The shortcut lemmas are not applicable to irregular terrains due to the anisotropism introduced by the special ranges. First of all, if there exists an impermissible range, an optimal path p_{opt} may choose to zigzag for an arbitrary number of times without losing its optimality, even if there is only one terrain face [see Fig. 6(a)]. Even if we consider only the optimal path with the minimum combinatorial size, this path may still have to zigzag an exponential number of times before reaching the destination point, if the impermissible range of a terrain face has an angle close to π. Therefore, the number of segments of an optimal path can only be bounded by the geometric parameters of the terrain faces.

However, since inside any terrain face, the face-wise optimal path between two points v and v' can be computed directly, we can treat each maximal subpath of p_{opt} that is face-wise optimal as one "virtual segment." The total error of an approximate optimal path of p_{opt} is not dependent on the number of segments of p_{opt}, but rather the number of virtual segments of p_{opt}, that is, the number of times p_{opt} switches from one region to another. In case there are multiple optimal paths from s to t, we are interested in only the optimal path with the fewest virtual segments. For example, on the surface of a pyramid with four identical faces [see Fig. 6(b)], an optimal path connecting a point at the bottom of the pyramid to a point near the apex can switch regions (faces) an infinite number of times while looping around the apex. However, there also exists another optimal path that stays in the same region while zigzagging toward the apex, and therefore has only one virtual segment.

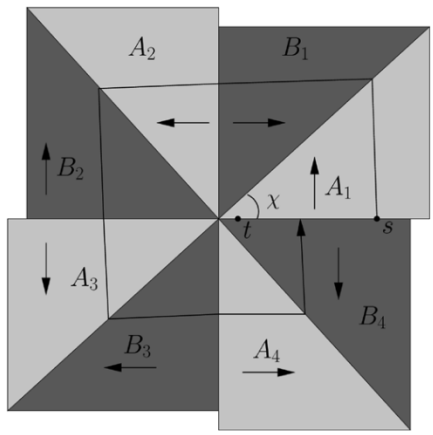

Fig. 7. Long path on irregular terrain.

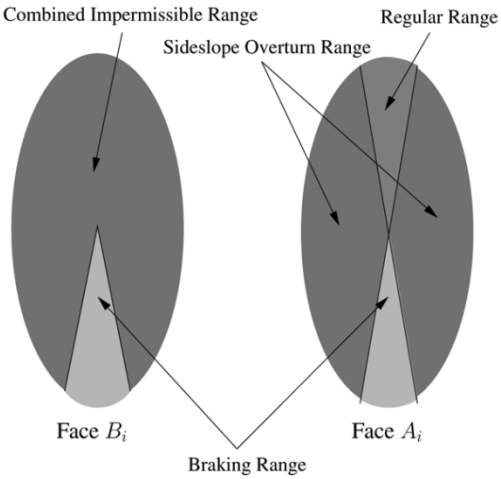

Fig. 8. Ranges of A_i and B_i.

For partially traversable terrains, we have the following theorem.

Theorem 2: If the input problem is specified with a total of N bits (i.e., the coordinates of all vertices are integers ranging from 0 to 2^N), for two points s and t on a partially traversable terrain, an optimal path with the fewest virtual segments, among all optimal paths that connect s and t, can contain $\Omega(2^{cN})$ virtual segments for some constant c.

Proof: As shown in Fig. 7, we construct an optimal-path problem on a partially traversable terrain with eight faces. In the figure, the arrow in each terrain face defines the upward direction in that terrain face.

Each A_i, with a gradient of ϕ_A and a friction coefficient of μ_A, is a totally traversable face. As shown in Fig. 8, there is no impermissible force range, and the two upward regular ranges combine into a single regular range with an angle of 2^{-c_2N} (radian measure). There is also a braking range with an angle of 2^{-c_2N}. We use $-\varphi_A$ to denote the inclination angle of the vector that separates the braking range and each of the two sideslope overturn ranges in A_i (and therefore, φ_A is the inclination angle of the vector that separates the regular range and the sideslope overturn ranges). Each B_i, with a gradient of ϕ_B and a friction coefficient of μ_B, is a partially traversable face. All four regular ranges are degenerate, resulting in a combined impermissible

range with an angle of $2\pi - 2^{-c_1 N}$ and a braking range with an angle of $2^{-c_1 N}$. Similarly, we let $-\varphi_B$ be the inclination angle of the vector that separates the braking range and the combined impermissible range in B_i.

Observe that in each terrain face A_i (B_i, respectively), the slope is steep enough so that the sideslope overturn ranges cover most parts of the braking range, and therefore, φ_A (φ_B, respectively) is not really determined by (2), but rather the boundary angles of the sideslope overturn ranges. In this case, φ increases as ϕ increases. From Fig. 7(a), it is easy to see that $\chi < (\pi/4)$, and therefore, $\phi_A > \phi_B$ and $\varphi_A > \varphi_B$.

An optimal path from s to t will contain alternating uphill and downhill segments. Each uphill segment is in a terrain face A with an inclination angle of φ_A. A downhill segment could only be one of the two cases: 1) a segment in a terrain face A with an inclination angle of $-\varphi_A$; or 2) a segment in a terrain face B with an inclination angle of $-\varphi_B$. Traveling in the braking range by an elevation decrease of h costs mgh in both A and B. (Recall that we remove the gravity cost factor from the cost function, and thus the cost of traveling inside the braking range is equal to the potential energy lost.) However, due to the fact that $\cos\chi > \sin\chi$ and that the braking range is larger in B than in A, a downhill segment in B can take the robot closer to the center of the terrain than a downhill segment in A. Therefore, it is more advantageous to move downhill in B and, as a result, an optimal path from s to t has to move counterclockwise, as shown in the figure. If we let $\tan\chi = 1 - 2^{c_3 N}$ for some constant c_3, each loop will take the robot $O(2^{-cN})$ closer to t for some constant c. Therefore, any optimal path from s to t will have to switch regions $\Omega(2^{cN})$ times. ■

Observe that we choose t to be a point very close to the center of the terrain. If t is located exactly at the center of the terrain, then the optimal path will only approach it asymptotically, but never reach there.

In the above construction, we used four partially traversable terrain faces. It occurs to us that such an example cannot be constructed without using partially traversable terrain faces. Therefore, we have the following conjecture.

Conjecture: For any two points s and t on a totally traversable terrain, there exists an optimal path connecting s and t with $O(n^2)$ virtual segments.

IV. An Improved Approximation Algorithm

A. Applicability of the BUSHWHACK Algorithm

Sun and Reif [20] defined *piecewise pseudo-Euclidean spaces* and showed that BUSHWHACK can be applied to any piecewise pseudo-Euclidean optimal-path problem. (For details of the BUSHWHACK algorithm, we refer readers to [20].) A space is said to be piecewise Euclidean if it consists of regions, each with a cost metric that satisfies the following two properties.

Property 2: ([20, Prop. 1]) Region r is associated with a cost function $d_r : (\mathcal{R}^2, \mathcal{R}^2) \rightarrow \mathcal{R}^+ \bigcup \{0\}$ so that, for any two points x and y in r, the cost of the straight-line path $\overline{xy}$ is $d_r(x, y)$. $d_r(x, y) = 0$ if and only if $x = y$. The cost function d_r has the property that the face-wise optimal path between x and y is the straight-line path $\overline{xy}$.

Property 3: ([20, Prop. 2]) Letting x_0 be a point in region r (including the boundary), and letting $e = \overline{v_0 v_1}$ be an edge of r that is not incident to x_0, there are only a small number of local extrema for function $g_{x_0,e} : [0,1] \rightarrow \mathcal{R}^+$, where $g_{x_0,e}(\lambda) \equiv d_r(x_0, (1-\lambda)v_0 + \lambda v_1)$. These local extrema can be computed efficiently.

Strictly speaking, a space defined by the physical model we study in this paper is not a piecewise pseudo-Euclidean space. Although it does satisfy *Property 3*, it does not satisfy *Property 2*: for two points v and v' inside terrain face r, if direction $\overrightarrow{vv'}$ is inside an impermissible range, straight-line segment $\overline{vv'}$ is not a valid path, and therefore, is not a face-wise optimal path between v and v'.

Nevertheless, BUSHWHACK is still applicable to the anisotropic optimal-path problem, as we will show in the following. We prove this by claiming that the following two lemmas hold for any terrain face r. The proof for *Lemma 3* is very trivial, and therefore, we only include the proof of *Lemma 4*.

Lemma 3: Letting v_1, v_2 be two Steiner points on a boundary edge e of r, for any other boundary edge e' of r, all Steiner points on e' can be divided into two subsets, I_1 and I_2, so that $\forall\, v^* \in I_1,\ d_r(v_1, v^*) + d_{\text{opt}}(s, v_1) \leq d_r(v_2, v^*) + d_{\text{opt}}(s, v_2)$ and $\forall\, v^* \in I_2,\ d_r(v_1, v^*) + d_{\text{opt}}(s, v_1) \geq d_r(v_2, v^*) + d_{\text{opt}}(s, v_2)$, where $d_{\text{opt}}(s, v)$ denotes the cost of an optimal path from s to v. Furthermore, for any $v_1^* \in I_1, v_2^* \in I_2$, straight-line segments $\overline{v_1 v_1^*}$ and $\overline{v_2 v_2^*}$ do not intersect with each other.

Lemma 4: For any fixed point v on boundary edge e of a terrain face r, each boundary edge e' of r can be divided into two monotonic segments, so that in each such segment, $d_r(v, x)$ is a monotonic function. Also, the split point can be computed in constant time.

Proof: Without loss of generality, we can assume that r is a triangular region with vertices A, B, and C. Let e be $\overline{BC}$, and let e' be $\overline{AC}$. Supposing there are k critical angles between $\overrightarrow{vA}$ and $\overrightarrow{vC}$, let $v_1^*, v_2^*, \ldots, v_k^*$ be points on $\overline{AC}$ so that each $\overrightarrow{vv_i^*}$ is a critical angle for $i = 1, 2, \ldots, k$. Additionally, we let $v_0^* = A$ and $v_{k+1}^* = C$. Let point v_h be the perpendicular point of v on boundary edge $\overline{AC}$, and let $[v_d^*, v_{d+1}^*]$ be the segment that contains v_h.

If $\overrightarrow{vv_d^*}$ and $\overrightarrow{vv_{d+1}^*}$ are the boundaries of a regular range, then $d_r(v, x)$ has a local minimum at v_h, as $d_r(v, x)$ is proportional to $|\overline{vx}|$ inside a regular range. If $\overrightarrow{vv_d^*}$ and $\overrightarrow{vv_{d+1}^*}$ bound an impermissible range or the braking range, according to *Property 1*, $d_r(v, x)$ is proportional to the projection of $\overline{vx}$ onto direction $\overrightarrow{vu_d^*}$, where u_d^* is the intersection point of boundary edge $\overline{AC}$ and the ray bisecting the range. If $\angle v u_d^* v_{d+1}^* < (\pi/2)$, then v_{d+1}^* is a local minimum; otherwise v_d^* is a local minimum.

Similarly, we can prove that function $d_r(v, x)$ is decreasing (respectively, increasing) when x moves from v_i^* to v_{i+1}^* for $0 \leq i < d$ (respectively, $d < i \leq k$). Therefore, function $d_r(v, x)$ has only one local extremum between A and C, which is the local minimum between v_d^* and v_{d+1}^*, as $d_r(v, x)$ is a continuous function. With this local minimum point, $\overline{AC}$ can be divided into two monotonic segments. And from the above discussion, it is also clear that this local minimum point can be computed efficiently in constant time.

Observe that in the above, we assume that v_h is between A and C. If v_h is not between A and C, we can prove with an

analogous argument that either there is no local minimum point between $\overline{AC}$, or there is only one local minimum point.

This finishes the proof. ■

Lemma 3 shows that the Steiner points on e' can be divided into intervals of contiguous Steiner points, so that an optimal discrete path $p'_{\text{opt}}(s, v)$ from s to $v \in e$ only needs to be propagated to Steiner points inside the interval associated with v. *Lemma 4* guarantees that the cost metric in each terrain face satisfies *Property 3*, and thus paths generated by extending $p'_{\text{opt}}(s, v)$ to those Steiner points can be sorted in linear time. Therefore, the above two lemmas are sufficient to show that BUSHWHACK can be applied to finding an optimal discrete path in $\mathcal{G}$ constructed from any discretization of a problem instance of the anisotropic optimal-path problem.

B. Discretization With Reduced Size

The uniform discretization does not guarantee a relative (multiplicative) error bound for the approximation. Lanthier *et al.* [16] developed a logarithmic discretization scheme that guarantees a $O(\epsilon')$-approximation for any optimal path. Here $\epsilon' = (w_{\max}\epsilon)/(w_{\min}\cos(\alpha_{\max}/2))$, where $\alpha_{\max}$ is the maximum angle of all special ranges, and $w_{\max}$ ($w_{\min}$, respectively) is the maximum (minimum, respectively) weight of all terrain faces. To achieve this error bound, the discretization needs to place $O(\log_{\delta_{\min}}(L/R) + \log_{\mathcal{F}}(R/L))$ Steiner points on each boundary edge. Here L is the length of the longest boundary edge, and $\delta_{\min} = 1 + \epsilon\sin\theta_{\min}$, where $\theta_{\min}$ is the minimum angle between any two adjacent boundary edges of any terrain face. For each vertex v, let $f_1, f_2, \ldots, f_d$ be the faces incident to v, and let h_v be the minimum distance between v and boundary edges of f_i's not incident to v. We let $r_v = \epsilon \cdot h_v$ and R be the minimum of all r_v's. Furthermore, $\mathcal{F}$ is a parameter dependent on $\theta_{\min}$ and some other geometric parameters.

The discretization scheme proposed by [16] adds Steiner points in three stages. In Stage 1, Steiner points are placed using the algorithm of [7] to ensure that the Euclidean distance between any two adjacent Steiner points on a boundary edge is at most ϵ times the length of any face-crossing segment with one end between them. In Stages 2 and 3, some additional Steiner points are added for each of the braking and regular ranges.

In the following, we show that the Steiner points added in Stage 1 alone can guarantee the same error bound of $O(\epsilon')$. In [16], the following assumption is implicitly used, and we will use the same assumption here.

Assumption 1: Each terrain face r is totally traversable. Otherwise, the terrain face is considered to be nontraversable.

We first briefly describe the placement of Steiner points (we refer readers to [7] for details). Let $e = \overline{vu}$ be a boundary edge of a terrain face. The Steiner points $v_1, v_2, \ldots, v_k$ are placed from v to u on e in such a way that $|\overline{vv_i}| = r_v \cdot \delta^{i-1}$. Here δ is defined to be $1 + \epsilon\sin\theta_v$ if $\theta_v < (\pi/2)$, or $1 + \epsilon$ if otherwise, where θ_v is the smallest angle between any two incident boundary edges of v. We add Steiner points $u_1, u_2, \ldots, u_{k'}$ from u to v on e in an analogous manner.

To prove that the discretization can guarantee an $O(\epsilon')$-approximation, we need to show that, for any optimal path p_{opt} in the original space, we can construct an approximation path in $\mathcal{G}$ with a cost at most $(1 + O(\epsilon')) \cdot \|p_{\text{opt}}\|$.

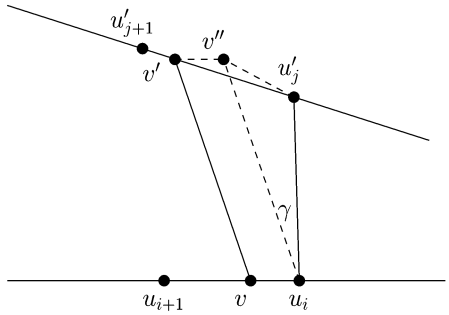

Fig. 9. Proof of *Lemma 5.4*.

Our construction of an approximation path is different from the one used in [16]. Suppose $\overline{vv'}$ is a segment of an optimal path ("optimal segment") in a terrain face r, where v is between two Steiner points u_1, u_2 on boundary edge e, and v' is between u'_1, u'_2 on boundary edge e'. The construction scheme in [16] will choose either $\overline{u_1u'_2}$ or $\overline{u_2u'_1}$, whichever is in the same directional range as $\overline{vv'}$, as the approximation segment for $\overline{vv'}$. The addition of Steiner points in Stages 2 and 3 is to guarantee that at least one of $\overrightarrow{u_1u'_2}$ and $\overrightarrow{u_2u'_1}$ is in the same directional range as $\overrightarrow{vv'}$. Observe that, according to this method, the approximation segments corresponding to two consecutive optimal segments are not necessarily connected. In this case, an additional "joint" segment, which connects two adjacent Steiner points, is added to the approximation path.

Our construction scheme does not require that an approximation segment be in the same range as the corresponding optimal segment. We show that the cost of an approximation segment can be bounded, regardless of its direction, by using the following lemma.

Lemma 5: For each $\overline{u_iu'_j}$, $i = 1, 2$ and $j = 1, 2$, we suppose $\overrightarrow{u_iu'_j}$ is in a range with an angle of α. Then:

1) if both $\overrightarrow{vv'}$ and $\overrightarrow{u_iu'_j}$ are inside the same regular range, then $d_r(u_i, u'_j) \le (1 + 2\epsilon) \cdot d_r(v, v')$;
2) if both $\overrightarrow{vv'}$ and $\overrightarrow{u_iu'_j}$ are inside the same impermissible range, then $d_r(u_i, u'_j) \le (1 + (2\epsilon)/(\cos(\alpha/2)) \cdot d_r(v, v')$;
3) if both $\overrightarrow{vv'}$ and $\overrightarrow{u_iu'_j}$ are inside the braking range, then $d_r(u_i, u'_j) \le (1 + (2\epsilon)/(\cos(\alpha/2))) \cdot d_r(v, v')$;
4) if $\overrightarrow{vv'}$ and $\overrightarrow{u_iu'_j}$ are not in the same range, then $d_r(u_i, u'_j) \le (1 + (3\epsilon)/(\cos(\alpha/2))) \cdot d_r(v, v')$ for $\epsilon \le (1/4)$.

Lemmas 5.1 and *5.2* are the same as the ones given by Lanthier *et al.* for their discretization scheme. *Lemma 5.3* is slightly stronger than the corresponding one in [16], but can be proved similarly (recall that $d_r(v, v')$ can be expressed in a unified form for impermissible ranges and braking ranges).

Lemma 5.4 is very important, as it allows us to bound the cost of an approximation segment even if the approximation segment is not in the same directional range as the corresponding optimal segment. We prove *Lemma 5.4* in the following.

Proof: (*Lemma 5.4*) Refer to Fig. 9. Let γ be the angle between $\overrightarrow{u_iu'_j}$ and $\overrightarrow{vv'}$. The placement of Steiner points added in Stage 1 guarantees that $\epsilon \cdot \min\{|\overline{vv'}|, |\overline{u_iu'_j}|\} \ge \max\{|\overline{u_iv}|, |\overline{v'u'_j}|\}$, and therefore, $\sin\gamma \le 2\epsilon$. In the following,

we assume that $(\alpha/2) \geq \gamma$. The case in which $(\alpha/2) < \gamma$ is trivial, and thus is omitted here.

Let v'' be the point such that $\overline{vv'} \| \overline{u_i v''}$ and $\overline{v'v''} \| \overline{vu_i}$. With a fixed γ, we can apply the "Law of Sines" twice on $\triangle u_i u'_j v''$, and obtain $\sin \angle u_i u'_j v'' = (|\overline{u_i v''}| \cdot \sin\gamma)/(|\overline{u'_j v''}|)$ and $|\overline{u_i u'_j}| = |\overline{u_i v''}| \cdot (\cos\gamma + \sin\gamma \cot \angle u_i u'_j v'')$. With $|\overline{u_i v''}| = |\overline{vv'}|$ and $|\overline{u'_j v''}| \leq |\overline{u'_j v'}| + |\overline{v'v''}| = |\overline{u'_j v'}| + |\overline{vu_i}| \leq 2\epsilon \cdot |\overline{vv'}|$, we have $|\overline{u_i u'_j}| \leq |\overline{vv'}| \cdot (\cos\gamma + \sqrt{4\epsilon^2 - \sin^2\gamma})$. On the other hand, since the angle between $\overrightarrow{u_i u'_j}$ and the boundary angle of the range containing $\overrightarrow{u_i u'_j}$ is at most γ, we have $d_r(u_i, u'_j) \leq mg \cdot w \cdot |\overline{u_i u'_j}| \cdot (\cos(\alpha/2 - \gamma))/(\cos(\alpha/2)) \leq d_r(v, v') \cdot (|\overline{u_i u'_j}|)/(|\overline{vv'}|) \cdot (\cos(\alpha/2 - \gamma))/(\cos(\alpha/2))$.

To give an upper bound to $(d_r(u_i, u'_j))/(d_r(v, v'))$, we first assume that $\sin\gamma \leq \lambda_0 \epsilon$, where $\lambda_0 = 1.49$. Therefore

$$\begin{aligned}
&\frac{d_r(u_i, u'_j)}{d_r(v, v')} \\
&\quad \leq (\cos\gamma + \sqrt{4\epsilon^2 - \sin^2\gamma}) \cdot \left(\cos\gamma + \tan\left(\frac{\alpha}{2}\right)\sin\gamma\right) \\
&\quad \leq (1 + 2\epsilon) \cdot \left(1 + \tan\left(\frac{\alpha}{2}\right) \cdot \lambda_0 \epsilon\right) \\
&\quad = 1 + \frac{2\cos\left(\frac{\alpha}{2}\right) + (1 + 2\epsilon)\lambda_0 \sin\left(\frac{\alpha}{2}\right)}{\cos\left(\frac{\alpha}{2}\right)}\epsilon \\
&\quad \leq 1 + \frac{\sqrt{4 + \lambda_0^2(1 + 2\epsilon)^2}}{\cos\left(\frac{\alpha}{2}\right)}\epsilon \\
&\quad \leq 1 + \frac{\sqrt{4 + 1.49^2\left(1 + 2 \cdot \frac{1}{4}\right)^2}}{\cos\left(\frac{\alpha}{2}\right)}\epsilon \\
&\quad = 1 + \frac{2.9992\epsilon}{\cos\left(\frac{\alpha}{2}\right)} \\
&\quad < 1 + \frac{3\epsilon}{\cos\left(\frac{\alpha}{2}\right)}.
\end{aligned}$$

Similarly, if $\sin\gamma > \lambda_0 \epsilon$

$$\begin{aligned}
&\frac{d_r(u_i, u'_j)}{d_r(v, v')} \\
&\quad \leq (\cos\gamma + \sqrt{4\epsilon^2 - \sin^2\gamma}) \cdot \left(\cos\gamma + \tan\left(\frac{\alpha}{2}\right)\sin\gamma\right) \\
&\quad \leq \left(1 + \sqrt{4 - \lambda_0^2} \cdot \epsilon\right) \cdot \left(1 + 2\epsilon \tan\left(\frac{\alpha}{2}\right)\right) \\
&\quad = 1 + \frac{2\left(1 + \sqrt{4 - \lambda_0^2} \cdot \epsilon\right)\sin\left(\frac{\alpha}{2}\right) + \sqrt{4 - \lambda_0^2}\cos\left(\frac{\alpha}{2}\right)}{\cos\left(\frac{\alpha}{2}\right)} \\
&\quad \leq 1 + \frac{\sqrt{4 - \lambda_0^2 + 4\left(1 + \sqrt{4 - \lambda_0^2} \cdot \epsilon\right)^2}}{\cos\left(\frac{\alpha}{2}\right)}\epsilon \\
&\quad \leq 1 + \frac{\sqrt{4 - 1.49^2 + 4\left(1 + \sqrt{4 - 1.49^2} \cdot \frac{1}{4}\right)^2}}{\cos\left(\frac{\alpha}{2}\right)}\epsilon \\
&\quad = 1 + \frac{2.9821\epsilon}{\cos\left(\frac{\alpha}{2}\right)} \\
&\quad < 1 + \frac{3\epsilon}{\cos\left(\frac{\alpha}{2}\right)}.
\end{aligned}$$

This finishes the proof. ∎

One difference between our path construction and the one used in [16] is that each of segments $\overline{u_1 u'_1}$, $\overline{u_1 u'_2}$, $\overline{u_2 u'_1}$, and $\overline{u_2 u'_2}$ can be used as an approximation segment for $\overline{vv'}$. We will pick a segment so that it is connected to the approximation segment corresponding to the previous optimal segment of $\overline{vv'}$. Therefore, we can avoid adding the "joint" segments, as the path construction in [16] does.

Recall that α_1, α_2, and α_3 are the angles of the impermissible force range, each sideslope overturn range, and the braking range, respectively. Combining *Lemma 5.1–5.4*, we have the following lemma.

Lemma 6: For each $\overline{u_i u'_j}, i = 1, 2$ and $j = 1, 2$, $d_r(u_i, u'_j) \leq (1 + (3\epsilon)/(\cos(\max\{\alpha_1/2, \alpha_2/2, \alpha_3/2\}))) \cdot d_r(v, v')$ for $\epsilon \leq (1/4)$.

This lemma is equivalent to the corresponding lemma in [16], although we achieve so without using Steiner points that they add in Stages 2 and 3.

In the above, we assume that the optimal segment is a face-crossing segment with each of the two endpoints between two Steiner points. For other types of optimal segments, we pick approximation segments in the same way as in [16], and their costs can be bounded in an analogous manner. Therefore, Steiner points added in Stage 1 can guarantee an $O(\epsilon')$-approximation. (Recall that $\epsilon' = (w_{\max}\epsilon)/(w_{\min}\cos(\alpha_{\max}/2))$. The extra factor $(w_{\max})/(w_{\min})$ is introduced for bounding approximation segments corresponding to other types of optimal segments.) As the number of Steiner points added in the first stage is $O(\log_{\delta_{\min}}(L/R))$ per boundary edge, we have the following result.

Theorem 3: An $O(\epsilon')$-approximation of an optimal anisotropic path can be computed in $O(nm' \log(nm'))$ time, where $m' = O(\log_{\delta_{\min}}(L/R))$.

This is an improvement over the result presented in [16], which has a time complexity of $O(nm^2 + nm\log(nm))$ with $m = O(\log_{\delta_{\min}}(L/R) + \log_{\mathcal{F}}(R/L))$. Not only does our algorithm reduce the size of the discretization (from $O(\log_{\delta_{\min}}(L/R) + \log_{\mathcal{F}}(R/L))$ to $O(\log_{\delta_{\min}}(L/R))$ Steiner points per boundary edge), but also, its time complexity is less dependent on the size of the discretization. As the size of the discretization is decided by not only the user-specified ϵ but also by a number of geometric parameters, it can be very large, even for a moderate ϵ.

V. Partially Traversable Terrain Faces

As mentioned above, we assume as in [16] that each terrain face is totally traversable. Here we briefly discuss the case in which partially traversable terrain faces are allowed.

In this case, the path-construction scheme described in the previous section may no longer be valid. Let v, v', u_1, u_2, u'_1, and u'_2 be defined as previously. Without loss of generality, we assume that the approximation segment for the previous optimal segment of $\overline{vv'}$ uses u_1 as one of its endpoints. It is possible that (as shown in Fig. 10) although $\overrightarrow{vv'}$ is a permissible direction, both $\overrightarrow{u_1 u'_1}$ and $\overrightarrow{u_1 u'_2}$ are inside the combined impermissible range. Therefore, neither $\overline{u_1 u'_1}$ nor $\overline{u_1 u'_2}$ can serve as the approximation segment for $\overline{vv'}$, as it is impossible to travel from u_1 to u'_1 and u'_2.

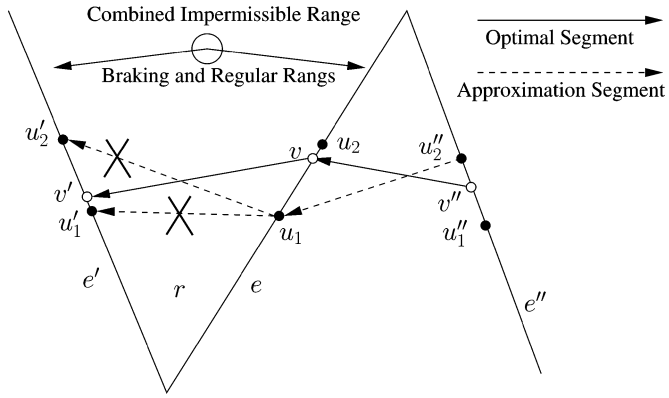

Fig. 10. No valid approximation segment.

To ensure that at least one approximation segment is available for each optimal segment, the discretization scheme needs to satisfy the following property.

Property 4: Let e and e' be two boundary edges of a partially traversable terrain face r. Let u_1 and u_2 (respectively, u_1' and u_2') be two adjacent Steiner points on e (respectively, e'). If there exist two points $v \in \overline{u_1u_2}$ and $v' \in \overline{u_1'u_2'}$ so that direction $\overrightarrow{vv'}$ is not inside the combined impermissible range, then for $i = 1, 2$ at least one of $\overrightarrow{u_iu_1'}$ and $\overrightarrow{u_iu_2'}$ is not inside the impermissible range, either.

To construct such a discretization, we need another stage, Stage 1.b, to add a series of additional Steiner points for each Steiner point added in Stage 1. Let $\overrightarrow{V_1}$ and $\overrightarrow{V_2}$ be the two boundary angles of the combined impermissible range. For any Steiner point v on boundary edge e of terrain face r, if the ray from v with direction $-\overrightarrow{V_i}, i = 1, 2$ intersects another boundary edge e' of r, we add the intersection point as a Steiner point on e'. We apply this rule to all Steiner points recursively until no more Steiner points can be generated.

Observe that the Steiner points spawned by v on boundary edge e (e', respectively) form a geometric series along e (e', respectively) with a ratio no less than $\mathcal{K} = (1 + \tan(\theta_{\min}/2)\tan(\alpha_{2,\min}/2))/(1 - \tan(\theta_{\min}/2)\tan(\alpha_{2,\min}/2))$, where $\alpha_{2,\min}$ is the minimum α_2 among all partially traversable terrain faces, and $\theta_{\min}$ is again the minimum angle between any two adjacent boundary edges of any terrain face. When both $\theta_{\min}$ and $\alpha_{2,\min}$ are small, $\mathcal{K}$ is asymptotically $1 + (\theta_{\min} \cdot \alpha_{2,\min})/(2)$. For a single Steiner point v added in Stage 1, there will be no more than $O(\log_{\mathcal{K}}(L/R))$ Steiner points spawned in Stage 1.b. This process is illustrated in Fig. 11.

It seems as though the total number of Steiner points required for this discretization is $O(n \log_{\mathcal{K}}(L/R) \cdot \log_{\delta_{\min}}(L/R))$. Recall that the Steiner points added on e in Stage 1 also form a geometric series, with a ratio no less than $\delta_{\min}$. By adjusting the ratio properly, we can substantially reduce the number of Steiner points added in Stage 1.b, as most of the Steiner points spawned will coincide with existing Steiner points. Therefore, the number of Steiner points generated can be bounded, as shown in the following.

Theorem 4: To construct a discretization that guarantees an $O((w_{\max}\epsilon)/(w_{\min}\cos(\alpha_{\max}/2)))$-approximation for the case

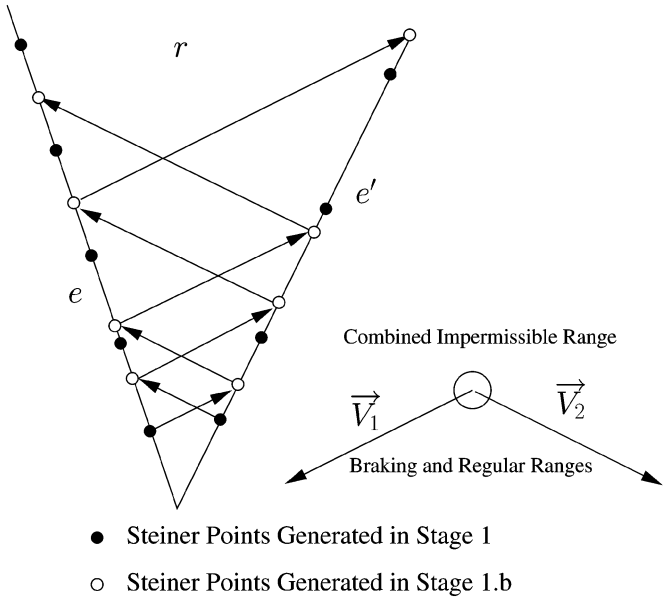

Fig. 11. New Steiner points added in Stage 1.b.

in which partially traversable terrain faces are allowed, the total number of Steiner points required is $O(n \log_{(\delta_{\min}+1)/2}(L/R))$ if $\mathcal{K} > \delta_{\min}$, or $O(n \log_{\mathcal{K}}(L/R))$, otherwise.

VI. Experimental Results

To compare the performance of our approximation algorithm described in Section IV with that of the previous work, we implemented both algorithms using Java. The experimental results were acquired from a Linux workstation with a 2.6-GHz Pentium processor and 2 GB memory.

A. Experiment Setup

One dilemma we faced in presenting experimental results is the choice of experimental data. On one hand, we prefer real data, as a randomly generated terrain may have an unexpected impact on the performance of the algorithms. On the other hand, we want to avoid terrain maps modeled using triangular irregular networks (TINs). Recall that, for a given terrain of n faces and a user-defined ϵ, the size of the resulting discretization is dependent on not only ϵ and n, but also a number of other geometric characteristics. Therefore, in an experiment on a group of TINs, one TIN with some extremely skewed triangular faces may produce more Steiner points than all other TINs combined, and therefore, the running time of an algorithm on this TIN will undesirably dominate the result of the entire experiment.

We chose to use triangular meshes generated from a digital elevation map (DEM). The advantage of using such triangular meshes is that each triangular face will not be too skewed, as its projection on the $x - y$ plane is an isosceles right triangle. For our experiment, we used the map of the Kaweah River basin in DEM ASCII format, which is a 1424×1163 grid with 30 m between two neighboring grid points. We took from the map 20 different 60×45 patches, and converted each of them into a triangular terrain by connecting two grid points diagonally for each grid cell.

We used the example of a car-like robot with a specific shape. The dimension of the robot is considered to be insignificant,

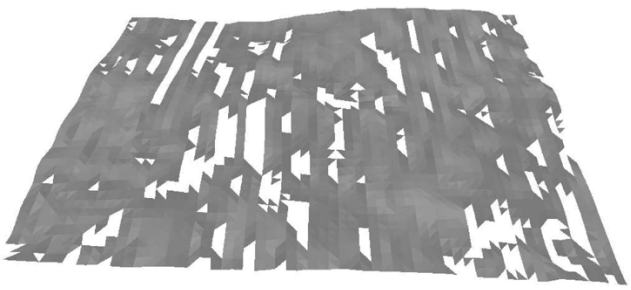

Fig. 12. Terrain map of Kaweah River basin.

as compared with that of the terrain, but the ratio between the height and width, which is chosen to be 2:1, is used to compute the sideslope overturn range for any given terrain face. We also defined the maximum driving force of the robot.

A friction coefficient is randomly picked for each terrain face, but only from a small range, again, to avoid producing skewed data. One major difference from the previous experiments (see [22]) is that here, we will intentionally pick friction coefficients to avoid, as much as possible, noninteresting terrain faces with no special ranges. Therefore, the terrains generated are more "difficult" than the ones used in the previous experiments, in the sense that they are more different from the weighted terrains.

With the friction coefficient and the maximum driving force, we can compute for each terrain face the impermissible force range, as well as the braking range. We refer readers to Appendix B for details on computing various special ranges for a given robot on a given terrain face.

For each generated terrain, we first remove all partially traversable faces, as both our algorithm and the algorithm of [16] assume no partially traversable faces. We also remove all vertices and boundary edges that are only incident to partially traversable faces. The numbers of remaining vertices (boundary edges, respectively) of the 20 terrains range from 1988 to 2670 (from 4668 to 7631, respectively), with an average of 2435 (6439, respectively). Fig. 12 shows one of the resulting terrains. Finally, we handpicked the points closest to the upper left and lower right corners as source and destination points, respectively.

B. Experimental Results

For $\epsilon = (1/4), (1/8), (1/12), (1/16)$, and $(1/20)$, we timed the performance of the two approximation algorithms, Algorithm 1, which uses BUSHWHACK along with the reduced discretization method described in Section IV-B, and Algorithm 2, as presented in [16], which uses Dijkstra's algorithm along with the original discretization method. Either algorithm is guaranteed to find an $(w_{\max}\epsilon)/(w_{\min}\cos(\alpha_{\max}/2))$-good approximate optimal path. The results for each algorithm are averaged over 20 runs, one for each terrain, and reported in Table I. Note that the running times were acquired from a Java implementation. So the relative performance is more important than the absolute values of running times.

First of all, Table I shows that for the two algorithms we used in the experiments, the difference in the number of Steiner points generated is relatively marginal. This difference is exactly the number of Steiner points generated in Stages 2 and 3 of the original discretization method [16]. This is due to the nature of the terrains used, which do not contain skewed terrain faces. If there exist extremely skinny triangular faces with very small regular or braking ranges, there will be a large number of Steiner points generated in Stages 2 and 3. Secondly, the difference becomes less significant as ϵ decreases. This is consistent with our analysis, as the number of Steiner points generated in Stages 2 and 3 depends less on ϵ than the number of Steiner points generated in Stage 1.

TABLE I
PERFORMANCE STATISTICS

$\frac{1}{\epsilon}$	Algorithm	Running Time (in sec.)	Steiner Points	Steiner Points per Boundary Edge	Touched Graph Edges
4	Alg. 1	14.54	105620	16.39	1918478
	Alg. 2	23.85	136484	21.16	5108645
8	Alg. 1	42.03	294696	45.74	5724099
	Alg. 2	132.67	353494	54.85	29959933
12	Alg. 1	76.69	519868	80.69	10473719
	Alg. 2	355.85	597349	92.73	82014045
16	Alg. 1	116.28	769324	119.42	15879714
	Alg. 2	712.40	861802	133.80	167013137
20	Alg. 1	165.93	1036751	160.93	21818934
	Alg. 2	1233.02	1142234	177.36	289649049

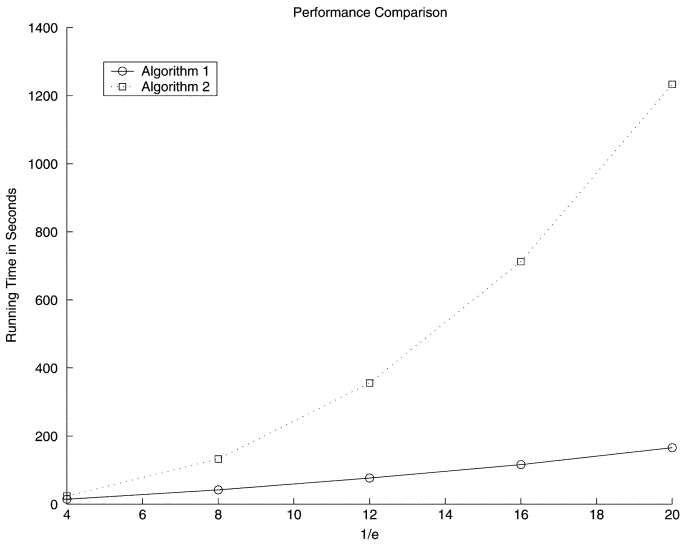

Fig. 13. Performance comparison (with respect to $1/\epsilon$).

The difference in the performance of the two approximation algorithms is, therefore, mainly caused by the difference in the efficiency of the discrete algorithms adopted for computing optimal discrete paths in $\mathcal{G}$. Fig. 13 shows a comparison between Algorithms 1 and 2 on the average running time (excluding time used for discretization). Note that the advantage of Algorithm 1 becomes more significant as ϵ decreases, a finding consistent with the fact that the time complexity of BUSHWHACK is less dependent on ϵ than the standard Dijkstra-based algorithm is. Fig. 14 shows that, as ϵ decreases, the increase of the speedup ratio (defined by the ratio between the running time of Algorithm 2 and that of Algorithm 1) correlates to the increase of the ratio of the number of graph edges touched in $\mathcal{G}$, supporting the analysis that BUSHWHACK outperforms the Dijkstra-based algorithm by accessing a small subset of graph edges in $\mathcal{G}$.

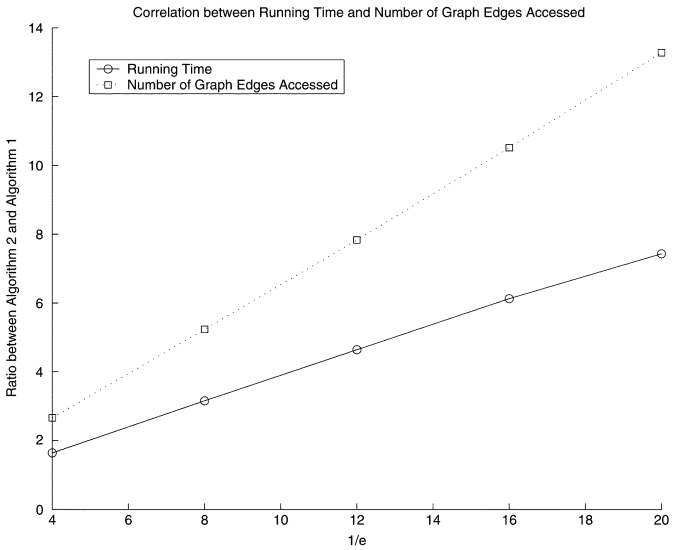

Fig. 14. Correlation between running time and number of graph edges accessed (with respect to $1/\epsilon$).

VII. Conclusion and Future Work

In this paper, we studied the energy-minimizing path problem. We provided some complexity results on the combinatorial size of energy-minimizing paths under various assumptions. We also presented an improved approximation algorithm using a smaller discretization, as well as a more efficient discrete search algorithm. Our preliminary experimental results show that our algorithm has a significant performance improvement over the previous algorithm when ϵ is small.

One remaining question is the complexity of the combinatorial size of energy-minimizing paths on totally traversable terrains. We believe that the upper bound should be $\Omega(n^2)$, the same as that of the weighted terrains, although proving so seems to be very hard.

We also plan to extend our experimentation work. In particular, we would like to study the impact of the improved discretization method on TINs. Imaginably, for a given ϵ, a TIN that contains skewed triangular faces may require significantly more Steiner points than does a triangular mesh generated from DEM. The efficiency of our approximation algorithm could become more evident due to the following two reasons: a) the size of discretization of our algorithm is less dependent on various geometric parameters and b) the complexity of our algorithm is less dependent on the number of Steiner points per boundary edge.

Appendix

A. Proofs of Two Shortcut Lemmas

Before providing the modified proofs for the two lemmas, we first introduce some notations. Let f_1 and f_2 be two adjacent terrain faces, and let e be the boundary edge between them. For an optimal path $p_{\rm opt}$ from s to t, we say point x is an "up-crossing" ("down-crossing," respectively) point of p on boundary edge e if p is directed from f_1 to f_2 (f_2 to f_1, respectively) when crossing e at x. We say two subpaths of p are homotopic if they pass through the same sequence of boundary edges. Again, we use $||p||$ to denote the weighted length of any path (subpath) p. If a and b are two points on p, we use $p[a,b]$ to denote the subpath of p that is between a and b.

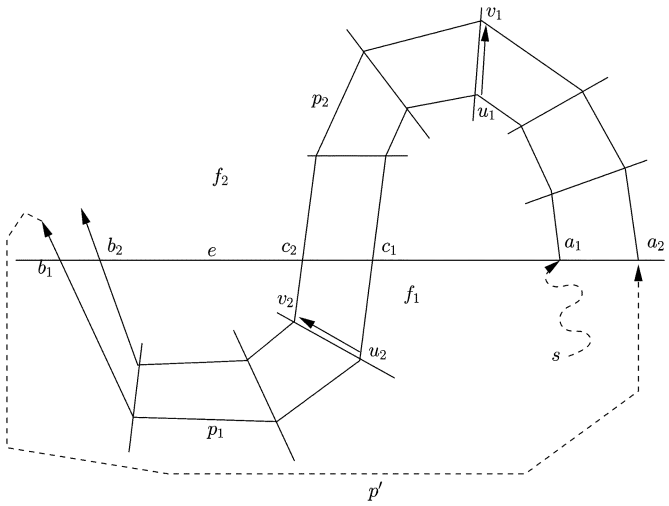

Fig. 15. Proof of *Lemma 7*.

We rephrase the two lemmas slightly so that readers can still understand them without referring to [4].

Lemma 7: Let p_1 and p_2 be two homotopic subpaths of $p_{\rm opt}$. Further, for each p_i, the two endpoints of p_i, namely, a_i and b_i, are up-crossing points on e, while between them there is a down-crossing point on e, denoted by c_i. If p_1 precedes p_2 along p, then it is not possible for a_1 and c_1 to be between a_2 and c_2, and for c_2 and b_2 to be between c_1 and b_1.

Proof: If otherwise, then p_1 and p_2 must be crossing boundary edge e in the way shown in Fig. 15. Since p_1 and p_2 are homotopic, $p_1[a_1,c_1]$ must be homotopic to $p_2[a_2,c_2]$, and $p_1[c_1,b_1]$ must be homotopic to $p_2[c_2,b_2]$. Let $\overline{u_1v_1}$ ($\overline{u_2v_2}$, respectively) be a chord joining $p_1[a_1,c_1]$ to $p_2[a_2,c_2]$ ($p_1[c_1,b_1]$ to $p_2[c_2,b_2]$, respectively) in the cheapest terrain face that $p_1[a_1,c_1]$ and $p_2[a_2,c_2]$ ($p_1[c_1,b_1]$ and $p_2[c_2,b_2]$, respectively) pass through.

Since p_1 precedes p_2 along optimal path $p_{\rm opt}$, there must be a subpath p' of $p_{\rm opt}$ that connects b_1 to a_2. We construct a path $p^1_{\rm opt}$ from $p_{\rm opt}$ by replacing the subpath of $p_{\rm opt}$ between u_1 and v_1 by "shortcut" $\overline{u_1v_1}$. Similarly, we construct $p^2_{\rm opt}$ by replacing the subpath of $p_{\rm opt}$ between u_2 and v_2 by $\overline{u_2v_2}$. We have the following equations regarding the weighted lengths of $p^1_{\rm opt}$ and $p^2_{\rm opt}$:

$$\begin{aligned}\left\|p^1_{\rm opt}\right\| &= \|p_{\rm opt}\| + \|\overline{u_1v_1}\| - \|p_1[u_1,b_1]\| \\ &\quad - \|p'\| - \|p_2[a_2,v_1]\| \qquad (3)\\ \left\|p^2_{\rm opt}\right\| &= \|p_{\rm opt}\| + \|\overline{u_2v_2}\| - \|p_1[u_2,b_1]\| \\ &\quad - \|p'\| - \|p_2[a_2,v_2]\|. \qquad (4)\end{aligned}$$

Therefore, we have

$$\begin{aligned}&\left\|p^1_{\rm opt}\right\| + \left\|p^2_{\rm opt}\right\| - 2\|p_{\rm opt}\| \\ &\quad = (\|\overline{u_1v_1}\| - \|p_1[u_1,b_1]\| - \|p'\| - \|p_2[a_2,v_1]\|) \\ &\qquad + (\|\overline{u_2v_2}\| - \|p_1[u_2,b_1]\| - \|p'\| - \|p_2[a_2,v_2]\|) \\ &\quad < \|\overline{u_1v_1}\| + \|\overline{u_2v_2}\| - \|p_1[u_1,b_1]\| \\ &\qquad - \|p_2[a_2,v_1]\| - \|p_1[u_2,b_1]\| - \|p_2[a_2,v_2]\| \\ &\quad = \|\overline{u_1v_1}\| + \|\overline{u_2v_2}\| - \|p_1[u_1,c_1]\| - \|p_1[c_1,b_1]\| \\ &\qquad - \|p_2[a_2,v_1]\| - \|p_1[u_2,b_1]\| - \|p_2[a_2,c_2]\| \\ &\qquad - \|p_2[c_2,v_2]\| \\ &\quad < (\|\overline{u_1v_1}\| - \|p_2[a_2,c_2]\| - \|p_1[u_1,c_1]\|) \\ &\qquad + (\|\overline{u_2v_2}\| - \|p_1[c_1,b_1]\| - \|p_2[c_2,v_2]\|).\end{aligned}$$

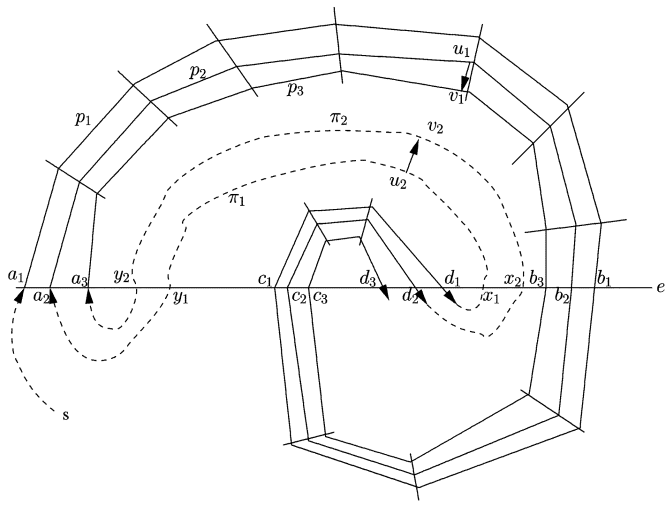

Fig. 16. Proof of *Lemma 8*.

According to *Lemma 2*, the Euclidean length of $\overline{u_1v_1}$ is less than the sum of the Euclidean lengths of $p_2[a_2, c_2]$ and $p_1[u_1, c_1]$. Further, because $\overline{u_1v_1}$ is inside the cheapest terrain face among all terrain faces that $p_2[a_2, c_2]$ and $p_1[u_1, c_1]$ travels through, we have $||\overline{u_1v_1}|| < ||p_2[a_2, c_2]|| + ||p_1[u_1, c_1]||$. Similarly, we can show that $||\overline{u_2v_2}|| < ||p_1[c_1, b_1]|| + ||p_2[c_2, v_2]||$, and hence, $||p^1_{\rm opt}|| + ||p^2_{\rm opt}|| < 2||p_{\rm opt}||$. This means that either $p^1_{\rm opt}$ or $p^2_{\rm opt}$ has a shorter weighted length than $p_{\rm opt}$, a contradiction to the assumption that $p_{\rm opt}$ is optimal.

Lemma 8: Suppose that p_1, p_2, and p_3 are three homotopic subpaths of $p_{\rm opt}$, and that p_1 precedes p_2, which precedes p_3 along $p_{\rm opt}$, as shown in Fig. 16. Each subpath p_i connects an up-crossing point a_i on e to a down-crossing point d_i, and also passes down-crossing point b_i and then up-crossing point c_i. Let π_1 (π_2, respectively) be the subpath of $p_{\rm opt}$ that connects p_1 and p_2 (p_2 and p_3, respectively). Let x_1 be the last up-crossing point of π_1 on e before it reaches a_2, and let y_1 be the last down-crossing point of π_1. Define x_2 and y_2 analogously. Then $\pi_1[x_1, y_1]$ and $\pi_2[x_2, y_2]$ cannot be homotopic.

Proof: Suppose otherwise that $\pi_1[x_1, y_1]$ and $\pi_2[x_2, y_2]$ are homotopic. Let $\overline{u_2v_2}$ be a chord through the cheapest region crossed by $\pi_1[x_1, y_1]$ and $\pi_2[x_2, y_2]$, joining $\pi_1[x_1, y_1]$ to $\pi_2[x_2, y_2]$. As p_2 and p_3 are also homotopic, we can find chord $\overline{u_1v_1}$ through the cheapest region crossed by $p_2[a_2, b_2]$ and $p_3[a_3, b_3]$, joining p_2 to p_3.

We construct a path $p^1_{\rm opt}$ from $p_{\rm opt}$ by replacing the subpath of $p_{\rm opt}$ between u_1 and v_1 by "shortcut" $\overline{u_1v_1}$. Similarly, we construct $p^2_{\rm opt}$ by replacing the subpath of $p_{\rm opt}$ between u_2 and v_2 by $\overline{u_2v_2}$. We have the following equations regarding the weighted lengths of $p^1_{\rm opt}$ and $p^2_{\rm opt}$:

$$\begin{aligned} \left||p^1_{\rm opt}|\right| &= ||p_{\rm opt}|| + ||\overline{u_1v_1}|| - ||p_2[u_1, d_2]|| \\ &\quad - ||\pi_2|| - ||p_3[a_3, v_1]|| \end{aligned} \tag{5}$$

$$\begin{aligned} \left||p^2_{\rm opt}|\right| &= ||p_{\rm opt}|| + ||\overline{u_2v_2}|| - ||\pi_1[u_2, a_2]|| \\ &\quad - ||p_2|| - ||\pi_2[d_2, v_2]||. \end{aligned} \tag{6}$$

Adding these two equations up, we have

$$\begin{aligned} &\left||p^1_{\rm opt}|\right| + \left||p^2_{\rm opt}|\right| - 2||p_{\rm opt}|| \\ &\quad = (||\overline{u_1v_1}|| - ||p_2[u_1, d_2]|| - ||\pi_2|| - ||p_3[a_3, v_1]||) \\ &\qquad + (||\overline{u_2v_2}|| - ||\pi_1[u_2, a_2]|| - ||p_2|| - ||\pi_2[d_2, v_2]||) \\ &\quad < ||\overline{u_1v_1}|| + ||\overline{u_2v_2}|| - ||\pi_2[x_2, y_2]|| \\ &\qquad - ||p_3[a_3, v_1]|| - ||\pi_1[u_2, y_1]|| - ||p_2[a_2, b_2]|| \\ &\quad = (||\overline{u_1v_1}|| - ||p_2[a_2, b_2]|| - ||p_3[a_3, v_1]||) \\ &\qquad + (||\overline{u_2v_2}|| - ||\pi_2[x_2, y_2]|| - ||\pi_1[u_2, y_1]||). \end{aligned}$$

Similar to the proof for *Lemma 7*, we can prove that $||\overline{u_1v_1}|| < ||p_2[a_2, b_2]|| + ||p_3[a_3, v_1]||$ and $||\overline{u_2v_2}|| < ||\pi_2[x_2, y_2]|| + ||\pi_1[u_2, y_1]||$. Therefore, $||p^1_{\rm opt}|| + ||p^2_{\rm opt}|| < 2||p_{\rm opt}||$, a contradiction to the assumption that $p_{\rm opt}$ is optimal. ■

We refer readers to [4] for the usage of these two lemmas, as well as the complete proof of the theorem.

B. Computing Special Ranges for a Terrain Face

We consider a car-like robot with a maximum driving force of $F_{\max}$. Suppose that the support points of the robot have a convex hull of a rectangle ("support rectangle") of width a and length b. Furthermore, for simplicity, we assume that the projection of the center of gravity of the robot onto the support rectangle is located at the geometric center of the rectangle, and use h to denote the distance between the center of gravity and the support rectangle.

Let r be a terrain face with a gradient of ϕ and a friction coefficient of μ. The two boundary angles of the impermissible force range can be determined by solving the following equation for φ:

$$\mu\cos\phi + \sin\varphi = F_{\max}. \tag{7}$$

If the above equation has a solution φ_1 such that $0 \le \varphi_1 \le \phi$, the size α_1 of the impermissible force range can be computed by

$$\cos\frac{\alpha_1}{2} = \frac{\sin\varphi_1}{\sin\phi} = \frac{F_{\max} - \mu\cos\phi}{\sin\phi}. \tag{8}$$

Otherwise, the impermissible force range is degenerate.

The two boundary angles of the braking range can be determined by solving the following equation for φ:

$$\mu\cos\phi + \sin\varphi = 0. \tag{9}$$

If the above equation has a solution φ_3 such that $-\phi \le \varphi_3 \le 0$, the size α_3 of the braking range can be computed by

$$\cos\frac{\alpha_3}{2} = \frac{-\sin\varphi_1}{\sin\phi} = \frac{\mu\cos\phi}{\sin\phi}. \tag{10}$$

Otherwise, the braking range is degenerate.

The size of each sideslope overturn range can be determined with the following equation:

$$\cos\frac{\alpha_2}{2} = \frac{a}{2h\cdot\tan\phi}. \tag{11}$$

Again, if there is no solution for this equation, the two sideslope ranges are degenerate.

For a totally traversable terrain face, the impermissible force range and the sideslope overturn ranges do not overlap, which implies that $(\alpha_1/2) + (\alpha_2)/(2) < (\pi)/(2)$, and thus,

$\cos^2(\alpha_1)/(2) + \cos^2(\alpha_2)/(2) > 1$. By substituting (8) and (11), we have

$$\left(\frac{F_{\max} - \mu\cos\phi}{\sin\phi}\right)^2 + \left(\frac{a}{2h\cdot\tan\phi}\right)^2 > 1 \qquad (12)$$

and therefore

$$\mu < \frac{F_{\max}}{\cos\phi} - \sqrt{\tan^2\phi - \frac{a^2}{4h^2}}. \qquad (13)$$

Similarly, for a totally traversable terrain face, we have $(\alpha_2)/(2) + (\alpha_3)/(2) < \pi$, as the braking range does not overlap with any of the two sideslope overturn ranges. Again, by substituting (10) and (11), we have

$$\left(\frac{\mu\cos\phi}{\sin\phi}\right)^2 + \left(\frac{a}{2h\cdot\tan\phi}\right)^2 > 1 \qquad (14)$$

and therefore

$$\mu > \sqrt{\tan^2\phi - \frac{a^2}{4h^2}}. \qquad (15)$$

REFERENCES

[1] N. C. Rowe and R. S. Ross, "Optimal grid-free path planning across arbitrarily contoured terrain with anisotropic friction and gravity effects," *IEEE Trans. Robot. Autom.*, vol. 6, pp. 540–553, Oct. 1990.

[2] R. Alexander and N. Rowe, "Path planning by optimal-path-map construction for homogeneous-cost two-dimensional regions," in *Proc. IEEE Int. Conf. Robot. Autom.*, 1990, pp. 1924–1929.

[3] N. C. Rowe and R. F. Richbourg, "An efficient Snell's law method for optimal-path planning across multiple two dimensional, irregular, homogeneous-cost regions," *Int. J. Robot. Res.*, vol. 9, no. 6, pp. 48–66, Dec. 1990.

[4] J. S. B. Mitchell and C. H. Papadimitriou, "The weighted region problem: Finding shortest paths through a weighted planar subdivision," *J. ACM*, vol. 38, no. 1, pp. 18–73, Jan. 1991.

[5] C. Mata and J. S. B. Mitchell, "A new algorithm for computing shortest paths in weighted planar subdivisions," in *Proc. 13th Annu. ACM Symp. Computat. Geom.*, 1997, pp. 264–273.

[6] M. Lanthier *et al.*, "Approximating weighted shortest paths on polyhedral surfaces," *Algorithmica*, vol. 30, no. 4, pp. 527–562, 2001.

[7] L. Aleksandrov, M. Lanthier, A. Maheshwari, and J.-R. Sack, "An ϵ-approximation algorithm for weighted shortest paths on polyhedral surfaces," in *Proc. 6th Scand. Workshop Algorithm Theory*, vol. 1432, 1998, pp. 11–22.

[8] J. H. Reif and Z. Sun, "An efficient approximation algorithm for weighted region shortest path problem," in *Proc. 4th Workshop Algorithmic Found. Robot.*, 2000, pp. 191–203.

[9] L. Aleksandrov, A. Maheshwari, and J.-R. Sack, "Approximation algorithms for geometric shortest path problems," in *Proc. 32nd Annu. ACM Symp. Theory Comput.*, 2000, pp. 286–295.

[10] ——, "An improved approximation algorithm for computing geometric shortest paths," in *Proc. 14th Int. Symp. Fundam. Computat. Theory*, vol. 2751, 2003, pp. 246–257.

[11] Z. Sun and J. H. Reif, "Adaptive and compact discretization for weighted region optimal path finding," in *Proc. 14th Int. Symp. Fundam. Computat. Theory*, vol. 2751, 2003, pp. 258–270.

[12] J. S. B. Mitchell, " Geometric shortest paths and network optimization," in *Handbook of Computational Geometry*, J.-R. Sack and J. Urrutia, Eds. Amsterdam, The Netherlands: Elsevier, 2000, pp. 633–701.

[13] J. P. Laumond, Ed., *Robot Motion Planning and Control*. ser. Lecture Notes in Control and Information Science. New York: Springer, 1998.

[14] N. C. Rowe and Y. Kanayama, "Near-minimum-energy paths on a vertical-axis cone with anisotropic friction and gravity effects," *Int. J. Robot. Res.*, vol. 13, no. 5, pp. 408–433, Oct. 1994.

[15] N. C. Rowe, "Obtaining optimal mobile-robot paths with nonsmooth anisotropic cost functions using qualitative-state reasoning," *Int. J. Robot. Res.*, vol. 16, no. 3, pp. 375–399, Jun. 1997.

[16] M. Lanthier, A. Maheshwari, and J.-R. Sack, "Shortest anisotropic paths on terrains," in *Proc. 26th Int. Colloq. Automata, Lang., Program.*, vol. 1644, 1999, pp. 524–533.

[17] J. H. Reif and Z. Sun, "Movement planning in the presence of flows," *Algorithmica*, vol. 39, no. 2, pp. 127–153, 2004.

[18] D. Gaw and A. Meystel, "Minimum-time navigation of an unmanned mobile robot in a 2-1/2D world with obstacles," in *Proc. IEEE Int. Conf. Robot. Autom.*, 1986, pp. 1670–1677.

[19] A. M. Parodi, "Multi-goal real-time global path planning for an autonomous land vehicle using a high-speed graph search processor," in *Proc. IEEE Int. Conf. Robot. Autom.*, 1985, pp. 161–167.

[20] Z. Sun and J. H. Reif, "BUSHWHACK: An approximation algorithm for minimal paths through pseudo-Euclidean spaces," in *Proc. 12th Annu. Int. Symp. Algorithms, Computat.*, vol. 2223, 2001, pp. 160–171.

[21] A. A. Rula and C. C. Nuttall, "An analysis of ground mobility models," U.S. Army Eng. Waterways Exp. Station, Tech. Rep. M-71-4, 1971.

[22] Z. Sun and J. H. Reif, "On energy-minimizing paths on terrains for a mobile robot," in *Proc. IEEE Int. Conf. Robot. Autom.*, 2003, pp. 3782–3788.

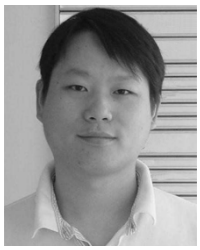

Zheng Sun (M'04) received the B.S. degree in computer science from Fudan University, Shanghai, China, in 1995, and the M.S. and Ph.D. degrees in computer science from Duke University, Durham, NC, in 1998 and 2003, respectively.

From 1999 to 2002, he was with Microsoft Corporation and Perfect Commerce as a Software Developer. In 2003, he joined the faculty of Hong Kong Baptist University, Kowloon, where he is an Assistant Professor of Computer Science. His research interests include robotic motion planning, computational geometry, and data mining and its applications in e-Commerce.

John H. Reif (S'77–M'78–SM'92–F'93) received the M.S. and Ph.D. degrees in applied mathematics in 1975 and 1977, respectively, from Harvard University, Cambridge, MA, and the B.S. degree (*magna cum laude*) in applied math and computer science in 1973 from Tufts University, Medford, MA.

He has been the Hollis Edens Distinguished Professor in the Trinity College of Arts and Sciences at Duke University, Durham, NC, since 2003, and Professor of Computer Science at Duke University since 1986. Previously he was an Associate Professor with Harvard University. Although originally primarily a theoretical computer scientist, he also has made a number of contributions to practical areas of computer science, including parallel architectures, data compression, robotics, and optical computing. He has also worked for many years on the development and analysis of parallel algorithms for various fundamental problems, including the solution of large sparse systems, sorting, graph problems, data compression, etc. He has developed algorithms and lower bounds for a large variety of robotic motion-planning problems, and provided the first known computational complexity results for a robotic motion-planning problem. He has also developed a wide range of efficient parallel algorithms, particularly randomized parallel algorithms. Recently, he has worked on DNA computing and DNA nanostructures. He is the author of over 200 papers and has edited three books on synthesis of parallel and randomized algorithms.

Dr. Reif has been a Fellow of Association for the Advancement of Science (AAAS) since 2003, a Fellow of the ACM since 1996, and a Fellow of the Institute of Combinatorics since 1991.